

Spin Effects in Processes of Single Top Quark Production at Hadron Colliders

E. E. Boos¹ and A. V. Sherstnev²

Skobeltsyn Institute of Nuclear Physics, Moscow State University,
119992 Moscow, Russia

Abstract

We investigate spin properties of single top quark production at hadron colliders. Based on an analogy with single top production and polarized top quark decay, we reproduce in a simple way the results by G. Mahlon and S. Parke on the existence of preferred axes for the decomposition of the top quark spin. For the W^* - and W - g -fusion production modes these axes are related to the down-type quark momentum. The proposed method allows finding kinematical conditions for the observation of top quark polarization in a third process that contributes to single top production and is important at LHC energies, the tW -process, in which spin effects are smeared out by the contribution of diagrams with a QCD $gt\bar{t}$ -vertex. A simple Monte-Carlo analysis of spin correlations for the tW -process with subsequent top decay is given as an illustration.

¹e-mail: boos@theory.sinp.msu.ru

²e-mail: sherstnv@theory.sinp.msu.ru

1 Introduction

The top quark is the heaviest Standard Model (SM) particle found so far, with a mass $m_t \sim 175 \text{ GeV} \sim v_H/\sqrt{2}$ (v_H - vacuum expectation of Higgs field) and with a Yukawa coupling very close to unity. This fact is probably related to a nature of the electroweak symmetry-breaking mechanism. In the SM the top quark is very heavy but at the same time is assumed to be point-like. Because of these and other unusual top quark properties, possible deviations from SM predictions might be first manifest in the top quark sector.

As a consequence of a large quark mass the top quark's electroweak decay $t \rightarrow W^- b$ (in the framework of SM) proceeds so rapidly that hadron bound states do not have enough time to form [1]. This leads to the fact that angular distributions of top quark decay products are mainly determined by the momentum and spin state of the t -quark itself and are not smeared out by hadronization effects [2].

Top quarks being produced singly through the electroweak interaction give a unique opportunity to investigate a number of delicate top quark properties. In particular, single top production is the only source of a direct measurement of the CKM matrix element V_{tb} . Because of the large production rate at hadron colliders, single t -quark production provides an important background to various processes expected in the SM and beyond, such as Higgs boson or SUSY particle production. Single t -quarks are expected to be produced with a high degree of polarization because of the pure (V-A)-structure of the production Wtb -vertex assumed in the SM. Spin properties of the all single top production processes are thus of special interest.

G. Mahlon and S. Parke have found that the direction of the spin of the single top quark in the production processes of W^* and W - g fusion coincides with the momentum of the down-type quark. For the W^* -process the down-type quark is the \bar{d} -quark in the initial state [3], while in W - g fusion it is either the final spectator quark (in the majority of events), or the \bar{d} -quark in the initial state [3], [4].

In this paper we show that the above results have a simple explanation if one considers single top production processes as decays of a polarized top quark considered backwards in time. By considering the analogy with polarized top decay, we find conditions for significant t -quark polarization in the third-most important single top production process at LHC energies, the so-called tW -process.

This paper is organized as follows. In Section 2 we mention briefly all three processes for single t -quark production at hadron colliders and recall the results obtained by G. Mahlon and S. Parke for the W^* -process and W - g fusion for top quark polarization. In Section 3 we give a simple explanation of these results based on properties of polarized t -quark decay and analyze spin polarization for the more complicated tW -process of single top production including subsequent top decay. A Monte-Carlo study of the t -quark spin effects in the tW -process is given in Section 4. The conclusions are presented in Section 5.

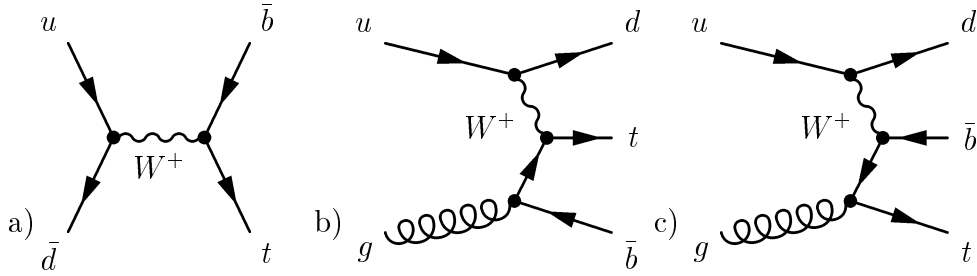


Figure 1: Typical diagrams for the W^* -process (a) and W - g fusion (b-c).

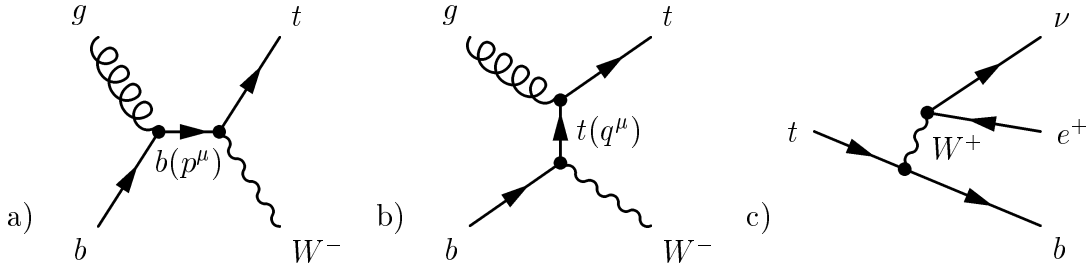


Figure 2: Diagrams for the tW -process (a-b) and LO t -quark decay (c).

2 Single Top Quark Production Processes

There are three SM processes of single top quark production at hadron colliders¹; some representative diagrams are shown in Figures 1 and 2(a-b)². Each of the processes may be characterized by the virtuality Q_W^2 , the four-momentum squared of the participating W -boson:

- t -channel W -exchange ($Q_W^2 < 0$): the characteristic diagrams are depicted in Fig. 1(b-c). This process has the largest cross section both at the Tevatron and LHC. It is referred as W - g fusion for the $2 \rightarrow 3$ diagrams shown, as well as for the $2 \rightarrow 2$ part with the b -quark in the initial state because the initial b -quark ultimately arises from a gluon splitting $g \rightarrow b\bar{b}$. We call the diagram 1(b) the Wtb -diagram because the top quark is produced at the Wtb -vertex. The diagram 1(c) is called the gtt -diagram. One should stress that for the $2 \rightarrow 2$ process there is only one Wtb -diagram.
- s -channel W -exchange ($Q_W^2 > 0$): the W^* -process. The characteristic diagram is depicted in Fig. 1(a). This process has a predicted rate for Run 2 at the Tevatron only about 2.5 times smaller than the W - g fusion rate. Although the process should be observable at the LHC, it has a cross section about 25 times smaller than the W - g fusion one (see the Table).

¹See the complete set of contributing parton subprocesses in [5].

²All Feynman diagrams in the paper were made with the help of the latex package feynmf written by T. Ohl [6].

Table 1: Total cross sections of single t -quark production processes for $m_t=175 \pm 2$ GeV [11].

process	W - g fusion	W^* -process	tW -process
LHC (pb)	245 ± 27	10.2 ± 0.7	$62.0 + 16.6 / - 3.6$
Tevatron (pb)	2.12 ± 0.1	0.88 ± 0.05	0.093 ± 0.024

- Real W production ($Q_W^2 = m_W^2$): tW -process. A single top quark appears in association with a real W -boson as shown in Fig. 2(a-b). These diagrams are also called the Wtb -diagram and gtt -diagram, depending on the type of the t -quark production vertex. This process has a very small production cross section at the Tevatron because of two massive particles in the final state, while at the LHC the rate is significant. We point out the presence of two Wtb - and gtt -diagrams even for the $2 \rightarrow 2$ part of the tW -process. As it will be shown this fact leads to additional complications for the analysis of the top quark spin properties.

The basic cross sections have been calculated to the NLO level in Ref. [7] for W - g fusion and in Ref. [8] for the W^* -process, and to LO for the tW -process in Ref. [9, 10] (see the Table).

Because of the unique (V-A) structure of the Wtb -vertex in the SM the electroweak single top production processes have very interesting top spin properties [3, 4, 12]. For the case of W^* - and W - g fusion, G. Mahlon and S. Parke [3, 4] have found rather compact formulae for single top production using a convenient formalism for top quark spin with an arbitrary spin direction. For the W^* -process it was shown the expressions for the squared matrix elements $|M(+)|^2$ ($|M(-)|^2$) for the top quark polarized along (opposite) some direction \vec{n}_t in its rest frame have a simple form ³

$$|M(+, u\bar{d} \rightarrow t\bar{b})|^2 = 9g_W^4 |V_{ud}V_{tb}|^2 \frac{(2d \cdot t_-)(2u \cdot b)}{(w^2 - m_W^2)^2 + (m_W \Gamma_W)^2}$$

for the spin up top quark and

$$|M(-, u\bar{d} \rightarrow t\bar{b})|^2 = 9g_W^4 |V_{ud}V_{tb}|^2 \frac{(2d \cdot t_+)(2u \cdot b)}{(w^2 - m_W^2)^2 + (m_W \Gamma_W)^2}$$

for the spin down top quark, where $t_+ = \frac{1}{2}(t + m_t s)$ and $t_- = \frac{1}{2}(t - m_t s)$. Spin vector of the top quark s^μ has a form $s^\mu = (0, \vec{n}_t)$ in the t -quark rest frame.

From these two formulas one can see that if one takes the polarization vector \vec{n}_t along the direction of the \bar{d} -quark three-vector momentum $\vec{p}_{\bar{d}}^*$ in the top rest frame,

$$\vec{n}_{\bar{d}} = \vec{p}_{\bar{d}}^* / p_{\bar{d}}^*,$$

the squared matrix element $|M(-, u\bar{d} \rightarrow t\bar{b})|^2$ exactly equals zero. G. Mahlon and S. Parke have interpreted this result in terms of the direction of the t -quark spin coinciding with

³As in [3, 4] we denote the momentum of the each particle by its symbol.

the direction of the \bar{d} -quark momentum ($\vec{s}_t \uparrow \uparrow \vec{p}_{\bar{d}}^*$). At the Tevatron the largest contribution to the total cross section comes from the case where the \bar{d} -quarks come from the antiproton. The best choice of the spin decomposition axis is thus the antiproton beam, which the authors call the “antiproton” spin basis.

The situation in the case of W - g fusion process is more complex. It was mentioned already long ago in the paper by Willenbrock and Dicus [13] that the W - g fusion process is dominated by the configuration where the \bar{b} quark from $g \rightarrow b\bar{b}$ splitting is nearly collinear with the incoming gluon, leading to a logarithmic factor $\ln(m_t^2/m_b^2)$ in the total cross section. It is well known that these large corrections are resummed, being absorbed into the b -quark parton distribution function. The correct LO rate is obtained then by summing up contributions of the $2 \rightarrow 2$ process $ub \rightarrow td$ and the $2 \rightarrow 3$ process mentioned above, with the subtraction of the first $g \rightarrow b\bar{b}$ splitting term in order to avoid double counting. The spin properties of the top quark in the $2 \rightarrow 2$ process, both in the subtracted term and in the dominant contribution of the $2 \rightarrow 3$ process coming from the Wtb -diagram, are similar in the top rest frame [4]. In all these cases the top is produced at the Wtb -vertex. The most effective spin decomposition axis is once more the direction \vec{n}_d^* . But the problem of extracting the d -quark momentum direction is less obvious now, because the d -quark appears both in the initial and final states. Two spin bases have been introduced here, the “spectator jet” basis related to the dominant single top contribution with the d -quark in the final state for the Tevatron and LHC, and the “ η -beamline” basis related to the d -quark in the initial state. The last is important for an analysis of \bar{t} -quark spin properties at the LHC.

In all cases the main spin effects are manifested in the simplest $2 \rightarrow 2$ processes with the b -quark in the initial state.

One remark is in order here. The fact that the top quark is polarized in the direction of \vec{n}_d^* means that $|M(+)|^2 \neq 0$ and $|M(-)|^2 = 0$. For the $2 \rightarrow 3$ diagrams of the W - g fusion shown in Fig. 1(b-c) the value of $|M(+)|^2$ comes from the contributions of all three parts, the Wtb , the $g\bar{t}t$ -diagrams and the interference between them. The Wtb -diagram and the interference do not contribute to $|M(-)|^2$. Indeed, one can show that if $\vec{n} = \vec{n}_d^*$ then $|M_{Wtb}(-, ug \rightarrow t\bar{b}d)|^2 = 0$ and the interference $M_{Wtb}(-) * M_{g\bar{t}t}^*(-) + h.c.$ is also exactly equal to zero. However, the $g\bar{t}t$ -diagram in general does not lead to any preferable direction of the top polarization, and gives nonzero contributions to both $|M(+)|^2$ and $|M(-)|^2$. Fortunately, $|M(-)|^2 = |M_{g\bar{t}t}(-, ug \rightarrow t\bar{b}d)|^2$ is much smaller than the complete $|M(+)|^2$, which comes from the large Wtb squared diagram and the interference. One can thus neglect the $|M(-)|^2$ part and conclude that with a good accuracy the top quark is polarized along the d -quark momentum in its rest frame.

For the tW mechanism of single top production the situation is similar in a sense that once more large corrections from the soft b -quark region are resummed by introducing the b -quark distribution function. This $2 \rightarrow 2$ contribution with the b -quark in the initial state dominates the production rate; top spin properties could therefore be studied by considering the $2 \rightarrow 2$ process. However, in contrast to the W - g fusion case, the $g\bar{t}t$ -diagram contribution to tW -process is significant and the corresponding diagram appears already in the $2 \rightarrow 2$ process as seen from the Fig. 2(a-b). The situation with top polarization in the tW -process thus requires special consideration.

3 Top Quark Polarization in the tW -process

In order to understand top quark spin properties in the tW -process it is useful to look at the results mentioned above for the W^* and W - g fusion processes from a different point of view.

The results on strong correlations between the t -quark spin and d -quark momentum can be obtained and explained in a very simple way based on the properties of polarized top decay. The diagram in Fig. 2(c) for the LO t -quark decay is topologically equivalent to the diagram for W^* -process and to the $2 \rightarrow 2$ part ($ub \rightarrow td$) of the W - g fusion (the latter reproduces the main features of the top spin properties in the complete W -gluon fusion as we mentioned). The decay matrix element is the same as that for production, and these processes differ only in the kinematical region over which they are integrated to get the decay width and the cross section. So the two single top production processes can be considered as a corresponding top decay backwards in time. The analogue of the d -quark in top decay $t \rightarrow l^+ \nu_l b$ is the charged lepton, since in the SM both the d -quark and the charged lepton are the down components of the electroweak doublets. Therefore the properties of the charged lepton from the decay should be similar to those of the d -quark.

The decays of polarized t -quarks have been investigated comprehensively many times both in LO and NLO [2], [14, 15, 16, 17]. The main result concerning the positron is that it is the best spin probe of the t -quark polarization [14]. The angular distribution of the positron from the decay of the top quark polarized along some axis \vec{n} in the t -quark rest frame is

$$\frac{1}{\Gamma} \frac{d\Gamma(\vec{s}_t \uparrow\uparrow \vec{n})}{d \cos \theta} = \frac{1 + \cos \theta}{2},$$

where θ is the angle between the t -quark spin direction \vec{n} and the momentum of the positron. So one gets unity for the distribution if the direction of the top polarization coincides with the positron momentum direction ($\theta = 0$) and zero for the opposite direction. In other words this means that for an arbitrary top polarization state along some direction, only the state with the projection along the positron momentum direction contributes to the decay.

One should stress that the existence of a preferred spin axis is related with the (V–A)-structure of the Wtb -vertex. In view of this fact a separation of one t -quark spin state does not cause astonishment. In some sense this situation is similar to the situation with the neutrino. A chiral projector P_L cuts out one helicity state of the neutrino. The top quark is the massive particle and its helicity and chirality states surely do not coincide. However, for the top the Wtb -vertex with exact (V–A)-structure leaves only the one spin projector of the t -quark in the non-polarized spin density matrix $P = p^\mu \gamma_\mu + m$. The interpretation is easiest in the t -quark rest frame, where $\vec{s}_t \uparrow\uparrow \vec{n}_{e^+}$.

Now returning back to the $2 \rightarrow 2$ production processes like $u\bar{d} \rightarrow t\bar{b}$ (W^*) or $ub \rightarrow td$ ($W - g$ fusion), and keeping in mind the analogy between the positron and the d -quark one can immediately conclude that the top quark is produced in a definite spin state with the top spin direction in its rest frame being along the \bar{d} or d quark momentum direction.

Also it becomes obvious that after top production with a definite polarization state only the projection of its spin state along the axis corresponding to the positron momen-

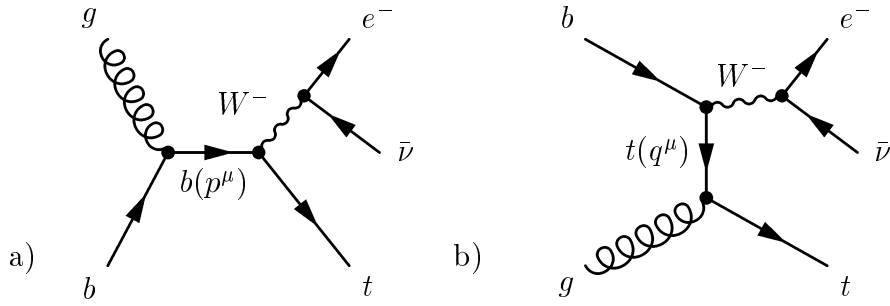


Figure 3: Diagrams of tW -process with decay of W -boson $W^- \rightarrow e^+\nu$

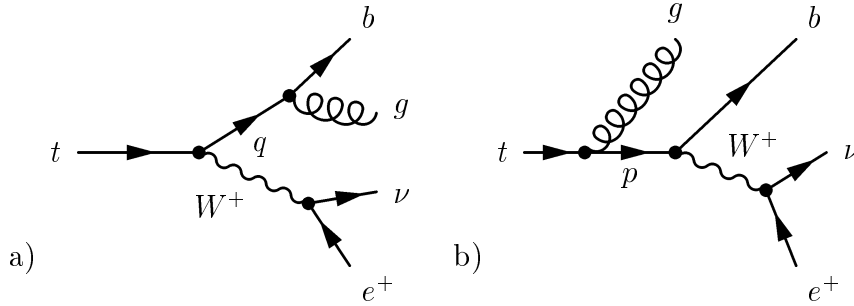


Figure 4: Diagrams of the decay $t \rightarrow b e^+ \nu + g$

tum as seen from the top rest frame contribute. Therefore the overall matrix element squared, including top production and decay, is proportional to $1 + \cos \theta_{e^+,d}^*$, where $\theta_{e^+,d}^*$ is the angle between the momenta of the positron and the d (or \bar{d})-quark in the top rest frame. The corresponding distribution has the form:

$$\frac{1}{\sigma} \frac{d\sigma}{d \cos \theta_{e^+,d}^*} = \frac{1 + \cos \theta_{e^+,d}^*}{2}$$

This result exactly reproduces the result by G. Mahlon and S. Parke discussed in the previous section, and corresponds to the highest possible spin correlation between production and decay. Correspondingly, the best variable for experimental analysis of the t -quark spin properties is $\cos \theta_{e^+,d}^*$.

Although the tW process, like the W^* -process or the W - g fusion part of the process with a b -quark in the initial state, is of the $2 \rightarrow 2$ type, there are two diagrams (Fig. 2a-b) and one of them is of the g tt -type. As we mentioned, in contrast to the W - g fusion the contributions of both these two diagrams are comparable in rate. One can not simply remove one of these two diagrams since only together do they form a gauge-invariant set of diagrams.

Let us consider how the analogy with the top decay helps in this case. If we add to the production diagram the leptonic decay of the W -boson produced in association with a top quark we get the diagrams presented in Fig. 3. The diagrams of the tW -process with W -boson decay in Fig. 3 are topologically equivalent to the diagrams of top quark decay with

radiation of an additional gluon $t \rightarrow be^+\nu + g$ (Fig.4), which is simpler to analyze. Let the axis for the top spin decomposition be the direction of the positron momentum produced in the W -boson decay, \vec{n}_e^* . Then one can easily check that the contribution of the Wtb -diagram squared to the top quark spin down configuration $|M_{Wtb}(-, t \rightarrow be^+\nu + g)|^2$ and the contribution of the Wtb - g t interference diagrams $|M_{Wtb^*g}(-, t \rightarrow be^+\nu + g)|$ equal to zero exactly in the same manner as it was for the W^* -process. However, the contribution of the g t t -diagram squared $|M_{g}(-, t \rightarrow be^+\nu + g)|^2$ does not vanish. It turns out that the contribution for polarized t -quark decay has a very simple symbolic structure

$$|M_{g}(-, t \rightarrow be^+\nu + g)|^2 = \frac{2g_s^2 g_W^2 |V_{tb}|^2}{(w^2 - m_W^2)^2 + (m_W \Gamma_W)^2} \frac{1}{(t \cdot g)^2} (b \cdot \nu) \left[m_t E_e^* E_g^{*2} (1 - \vec{n}_e^* \vec{n}_g^*)^2 \right],$$

where E_e^* and E_g^* are the energies of the positron and the gluon, and \vec{n}_e^* and \vec{n}_g^* are the directions of their 3-momenta in the top rest frame, respectively. However if the direction of the emitted gluon gets closer to the positron direction in the top quark rest frame, or if the energy of the gluon gets closer to zero, the g t t -diagram contribution, where $\vec{s}_t \uparrow \downarrow \vec{p}_e^*$, goes to zero as well. In the limit $\cos \theta_{e^-,g}^* \rightarrow 0$ the top quark will be produced with a definite spin direction along the positron momentum.

Now let us turn to the tW production process and the analogy with the radiative decay. From the above considerations it follows that in single top production in association with a W -boson (see Fig. 3) the top quark spin in its rest frame approaches 100% polarization along the momentum of the produced electron in the case when the electron momentum approaches the direction of the gluon. The same happens in the limit of zero gluon energy.

To get the cleanest top spin state, one should thus require the variable $\cos \theta_{e^-,g}^*$ to be as close as possible to unity. One can also apply an upper bound on the gluon energy in the top rest frame. We have found from MC studies that an excellent variable to cut on is a combination of these two quantities, $X_{g,e^-} = E_g^*(1 - \cos \theta_{e^-,g}^*)$.

Now if one considers the subsequent top quark decay we know already that only those projections of the top spin state contribute to the top decay which coincide to the direction of the positron from the top decay. Therefore from our considerations it follows that a good variable to probe spin properties of the top quark in the tW -process is the $\cos \theta_{e^-,e^+}^*$ where the electron comes from the W -boson decay produced in association with top, and the positron comes from the top decay.

4 Monte-Carlo Results

There are 4 modes to search for the tW -process, depending on the decay channels of the t -quark and W^- -boson. Taking into account t -quark spin, all of them are not equivalent.

dilepton channel: t -quark (W^+ boson from top decay) and W^- -boson decay to leptons.

One can determine easily the directions of the e^+ and e^- momenta. However, finding the t -quark rest frame is a problem because of the two neutrinos in the final state. If the 6 components of the neutrino momenta are introduced as unknown variables one gets only 5 equations: 2 equations from the measured missing P_T vector, and 3 equations from the 3 known masses, M_t and two M_W . An additional

condition can be obtained from the simultaneous measurement of the semileptonic mode with hadronic top decay, and consequently a normalization of the leptonic mode. However the accuracy of such a procedure needs to be studied in detail [18]. Also the production rate includes two small branching ratios $Br(W \rightarrow l\nu_l) = 2/9$ if l is an electron or muon, and $1/3$ if one includes τ in the analysis.

t-leptonic channel: top quark decays leptonically and W -boson – hadronically. Because of the analogy between the d -quark and the electron discussed in the previous section, the variable used for top spin analysis will be the angle between the positron from the top decay and the d -quark from the W decay. This mode also has a problem of the reconstruction of the t -quark rest frame, since one should extract the longitudinal part of the neutrino momentum solving the equation for the W -boson mass. Moreover, one needs to separate the d -quark jet from the u -quark jet from the decay $W^- \rightarrow d\bar{u}$ which is very problematic.

W-leptonic channel: top quark decays hadronically and W -boson – leptonically. In contrast to the t-leptonic channel, in the W-leptonic mode the t -quark rest frame could be easily extracted, but the problem of a separation of the \bar{d} -quark jet in the t -quark decay remains.

hadronic channel: Although this process does not have troubles with the top and W mass reconstruction the problem of d and \bar{d} jet separation from the corresponding \bar{u} and u jet remains and leads to additional uncertainties. Also the QCD background is very large in this case.

The complete MC analysis of the top spin properties in the tW -mode is a complicated problem and it is beyond the scope of this paper. We present here only some illustrative MC results for the dilepton channel, ignoring for the moment the problems of the top rest frame, reconstruction and contributions of backgrounds. The detail MC analysis including backgrounds will be presented elsewhere [18].

We have used the program package CompHEP [19] for the Monte-Carlo generation of tW -process events. The events are generated for a proton-proton initial state at the nominal LHC energy, $\sqrt{s} = 14$ TeV, using CTEQ5M1 structure functions [20].

The normalized distribution $d\sigma/d\cos\theta_{e^+,e^-}^*$ for the tW -process without any cuts is shown in Fig. 5 (dashed line). As was explained above, if one applies cuts on the variables $\cos\theta_{e^-,g}^* = \vec{n}_g^* \cdot \vec{n}_{e^-}^*$ and E_g^* in the top quark rest frame the degree of t -quark polarization of the event sample has to increase. Previously we mentioned the best variable here is the combination of the angle and gluon energy, of the form $X_{g,e^-} = E_g^*(1 - \cos\theta_{e^-,g^*})$. If the variable X_{g,e^-} is small enough, the $g\bar{t}t$ -diagram contribution is also small. The solid curve in Fig. 5 demonstrates a much higher spin correlation after the cut $X_{g,e^-} < 110$ GeV is applied.

It is useful to analyze the spin asymmetry R_{spin} , which is determined from the formula

$$\frac{1}{\sigma} \frac{d\sigma}{d\cos\theta_{e^+,s}^*} = \frac{1 + R_{spin}(\vec{s}) \cdot \cos\theta_{e^+,s}^*}{2}$$

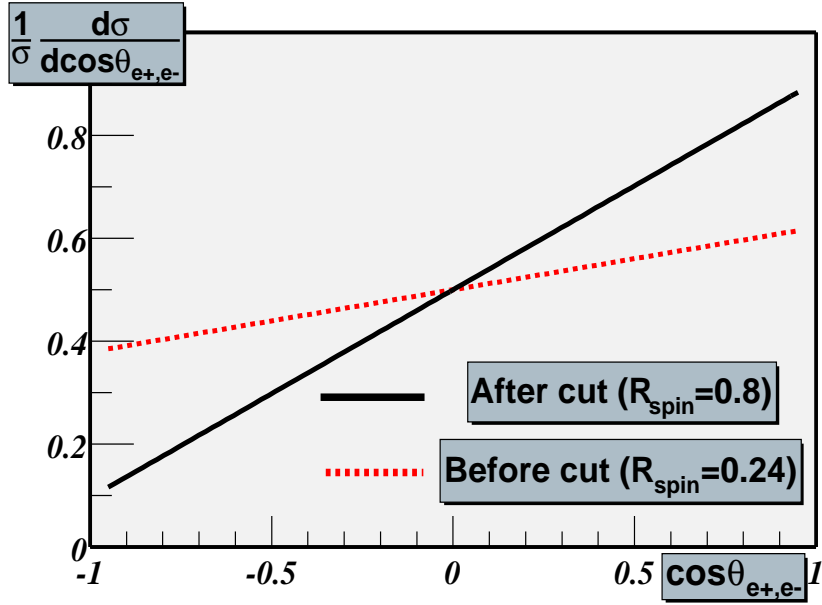


Figure 5: The normalized distributions $d\sigma/d\cos\theta_{e^+,e^-}^*$ for the tW -process: dashed line – without cuts, solid line – cut $X_{g,e^-} < 110$ GeV.

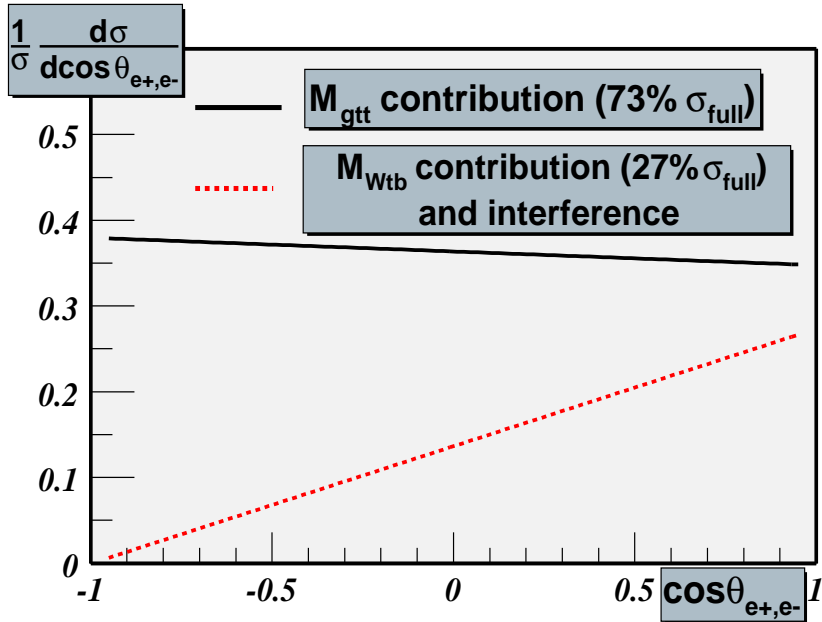


Figure 6: The normalized distributions $d\sigma/d\cos\theta_{e^+,e^-}^*$ for the $g\bar{t}t$ -diagram and the Wtb -diagram plus their interference.

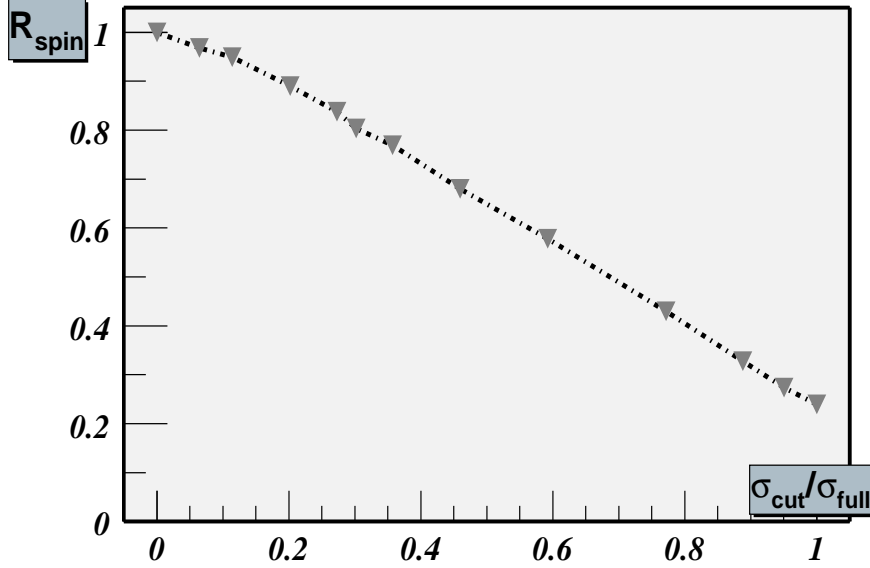


Figure 7: The spin asymmetry R_{spin} vs. the fall of the cross section for the tW -process with the X_{g,e^-} cut.

and changes between -1 to 1 for different spin axes. For a chosen spin axis \vec{s} along the electron momentum direction one can express the value of the spin asymmetry as

$$R_{spin} = \frac{y(1) - y(-1)}{y(1) + y(-1)}$$

where $y(x) = d\sigma/d \cos \theta_{e^+,e^-}^*$ and $x = \cos \theta_{e^+,e^-}^*$. If top quark would be fully polarized along the n_{e^-} direction the spin asymmetry R_{spin} would be equaled to 1.

In the case of the tW -process the spin asymmetry equals $R_{spin} \approx 0.24$. The smallness of R_{spin} is a result of the influence of the $g\bar{t}t$ -diagram. The individual diagram contributions in the t'Hooft-Feynman gauge are shown in Fig. 6. Although the contribution of the Wtb -diagram is large, the interference between Wtb - and $g\bar{t}t$ -diagrams is destructive and leads to a cancellation in the angular distribution. The $g\bar{t}t$ -diagram contribution is consequently the largest.

As it was explained above, in the limit $X_{g,e^-} \rightarrow 0$ the spin asymmetry approaches 1. In Fig. 5 the normalized angular distribution demonstrates the increase of the spin asymmetry from 0.24 to 0.8 if a proper cut on X_{g,e^-} is applied. With this cut tW -process cross section drops by a factor of 3. The dependence of R_{spin} on the cross section after the cut is shown in Fig. 7.

In order to increase the spin asymmetry R_{spin} one can also use properties of the distribution $d\sigma/d \cos \theta_{e^+,e^-}^*$ itself. From Fig. 6 we can see that the distribution of events from the Wtb squared diagram plus the interference has a peak near $\cos \theta_{e^+,e^-}^* = 1$. These events correspond to t -quarks which are fully-polarized along the e^- momentum. The distribution $d\sigma/d \cos \theta_{e^+,e^-}^*$ of events with the opposite top quark polarization has a peak

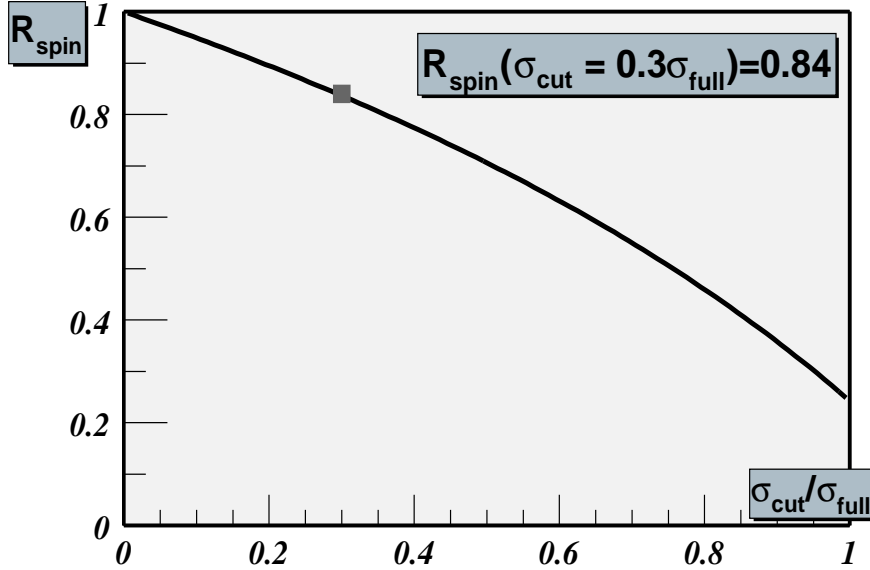


Figure 8: The spin asymmetry R_{spin} vs. the fall of the cross section of tW -process with the $\cos\theta_{e^-,e^+}^*$ cut.

near $\cos\theta_{e^+,e^-}^* = -1$. The contribution from the $g\bar{t}t$ squared diagram is almost flat, which means it gives about equal numbers of events with both top quark polarizations. Therefore, if one cuts out the region of $\cos\theta_{e^+,e^-}^*$ close to -1 , a significant fraction of the events with the opposite spin configuration will be removed. The Fig. 8 shows the increase of R_{spin} depending on the ratio of cross section after the $\cos\theta_{e^+,e^-}^*$ cut to the full one.

In practice in order to get an event sample with higher top polarization one can use cuts on both variables X_{g,e^-} and $\cos\theta_{e^+,e^-}^*$ simultaneously.

5 Conclusions

In the paper a close relation between spin properties in single top quark production and in polarized top quark decay has been pointed out. Based on the known fact that the positron in top decay $t \rightarrow be^+\nu_e$ is the best probe of the top spin, and on the analogy between the positron and the down-type quark, one can conclude the top quark spin in each event should follow the direction of the down-type quark momentum in the top quark rest frame. This is the direction of the initial \bar{d} -quark for the W^* -process, and the dominant direction of the final d -quark for the W - g fusion process. Also it becomes obvious that the best variable to observe maximal top spin correlations between the top production and subsequent decay is the angle between this down-type quark direction in the production processes and the charged lepton (or d -quark) direction from the top decay in the top rest frame.

Spin properties of the t -quark in a third production mechanism, the tW -process, are more complicated to analyze. In this case the diagram where the top quark is produced at the (QCD) $g\bar{t}t$ -vertex contributes with a significant rate in contrast to the two processes discussed earlier. The observed analogy of the tW production mode to radiative polarized top decay allows finding effective kinematical variables, e.g. X_{g,e^-} and $\cos\theta_{e^+,e^-}^*$, to reduce the contribution with the opposite polarization. Cuts on these variables select top quarks produced with the polarization vector preferentially close to the direction of the charged lepton or the d -quark momentum from the associated W decay. These cuts thus can raise the observed spin asymmetry R_{spin} in the process. We present a Monte-Carlo analysis only for the dilepton channel and at the parton level for final states. More realistic Monte-Carlo generation taking into account hadronization effects, identification of particles, and other detailed effects is in progress.

6 Acknowledgments

The authors are grateful to G. Belanger and F. Boudjema for useful discussions. This research was supported in part by CERN-INTAS grant 99-0377, INTAS grant 00-0679, and RFBR grant 01-02-16710. E.B. thanks the Bessel Research Award of the Humboldt Foundation.

References

- [1] I. Bigi, Y. Dokshitzer, V. Khoze, J. Kühn, and P. Zerwas, Phys. Lett. **B181** (1986) 157.
- [2] M. Jezabek and J.H. Kühn, Phys. Lett. **B329** (1994) 317.
- [3] G. Mahlon and S. Parke, Phys. Rev. **D55** (1997) 7249.
- [4] G. Mahlon and S. Parke, Phys. Lett. **B476**, (2000) 323.
- [5] A.P. Heinson, A.S. Belyaev, and E.E. Boos, Phys. Rev. **D56** (1997) 3114.
- [6] T. Ohl, Comput. Phys. Commun. **90**, (1995) 340.
- [7] M. C. Smith and S. Willenbrock, Phys. Rev. **D54**, (1996) 6696.
- [8] T. Stelzer, Z. Sullivan and S. Willenbrock, Phys. Rev. **D56** (1997) 5919.
- [9] T.P. Tait, Phys. Rev. **D61** (2000) 034001.
- [10] A.S. Belyaev and E.E. Boos, Phys. Rev. **D63** (2001) 034012.
- [11] M. Beneke, I. Efthymiopoulos, M.L. Mangano, J. Womersley et al., Top Quark Physics, in CERN'1999, Standard Model Physics (and more) at LHC, hep-ph/0003033.
- [12] T. Tait, C.-P. Yuan, Phys.Rev. **D63** (2001) 014018.

- [13] S. Willenbrock and D.A. Dicus, Phys. Rev. **D34**, (1986) 155.
- [14] M. Jezabek and J.H. Kühn, Nucl. Phys. **B320** (1989) 20.
- [15] J.H. Kühn, Lect. at XXIII SLAC Summer Institute, hep-ph/9707321 , and referances therein.
- [16] M. Fischer, S. Groote, J.P. Körner, M.C. Mauser, and B. Lampe, Phis. Lett. **B451** (1999) 406.
- [17] M. Fischer, S. Groote, J.P. Körner, and M.C. Mauser, hep/ph-0101322.
- [18] E. Boos and A. Sherstnev, detail Monte-Carlo analysis of the tW -process is in progress.
- [19] A.Pukhov et al., Preprint INP MSU 98-41/542, hep-ph/9908288.
- [20] CTEQ Collaboration (H.L. Lai et al.), Eur.Phys.J.C12:375-392, 2000.